Research article

The Journal of Computational Multiphase Flows

The Journal of Computational Multiphase Flows
2018, Vol. 10(2) 59–71

DOI: 10.1177/1757482X17746919
journals.sagepub.com/home/cmf
SAGE

Numerical simulation of bioaerosol particle exposure assessment in office environment from MVAC systems

HC Yu, KW Mui and LT Wong

Abstract

Bioaerosol (i.e. biological aerosol) exposures in the office environment are associated with a wide range of health effects. The potential bioaerosol emission from mechanical ventilation and air conditioning (MVAC) systems can endanger the building occupants in office, especially as over 90% of commercial buildings in Hong Kong that are equipped with MVAC systems, due to the microbial growths inside MVAC systems, such as cooling coils and mixing chamber, were reported. This study evaluated the exposure risk of the bioaerosol emission from the MVAC systems to the building occupants. A two-phase flow computational fluid dynamics approach was adopted to simulate the emission, dispersion, deposition, and exhaustion of bioaerosol particles from the MVAC systems in a typical office cubicle by altering the ventilation strategies with four ventilation rates, four emission concentrations, and two microorganism species. The results reported that about 5% contribution of concentration level from the MVAC system including the ventilation rate is sufficient to dilute the biocontainment. This study suggested the importance of the maintenance strategies of MVAC systems for minimizing bioaerosol exposures in offices.

Keywords

Bioaerosol particle, infection risk assessment, two-phase flow computational fluid dynamics simulation, ventilation rate, workplace

Date received: 29 June 2017; accepted: 14 November 2017

Introduction

Bioaerosol (i.e. biological aerosol) exposures in the office environment are associated with a wide range of health effects.[1] The microbial growths inside the mechanical ventilation and air conditioning (MVAC) systems, such as cooling coils, mixing chamber, air filters, air ducts, humidifiers, and heat exchangers, were reported.[2–6] For example, the bacterial concentrations were found up to 106 CFU cm^{-2} on the surfaces of the air-handling cooling coils.[5] The growths of biofilm have also been reported within heat exchangers that have the excess of 47,000 CFU cm^{-2} within four weeks of operation.[6] MVAC systems are likely to be reservoirs for microorganisms.

The existence of these microorganisms inside the MVAC systems can endanger the building occupants. The high potential of the microorganisms is aerosolized to form bioaerosol particles due to high airflow rate inside the MVAC systems.[4] The bioaerosol particles are then dispersed in the system and eventually into the occupied space through the air distribution system. For example, air samples taken at cooling coils and mixing chamber were recorded at 3880 and 865 CFU m^{-3} for the fungal and bacterial counts, respectively.[2] The dominant bacterial genera were *Micrococcus* spp., *Staphylococcus* spp., and *Bacillus* spp. For fungi, the dominant genera collected were *Aspergillus* spp., *Cladosporium* spp., *Penicillium* spp., and *Fusarium* spp. Various respiratory symptoms and health outcomes of the biocontaminated building

Department of Building Services Engineering, The Hong Kong Polytechnic University, Hong Kong, China

Corresponding author:
HC Yu, Department of Building Services Engineering, The Hong Kong Polytechnic University, Hong Kong, China.
Email: yu.ho.ching@connect.polyu.hk

occupants were reported, often implicated by elevated bioaerosol exposures.[7]

Little understanding of the relative influences of bioaerosol exposure from the MVAC systems to the building occupants was found. No study is available yet to assess quantitatively how bioaerosol emission occurs from the MVAC systems and other related factors and on how to evaluate the indoor bioaerosol concentrations in air-conditioned offices. One of the functions of the MVAC systems is to reduce the bioaerosol concentration level. Knowledge concerning the degree of connectivity between indoor and bioaerosol emission from the MVAC system is limited.[8] It is uncertain how the bioaerosol from the MVAC systems affects office workers in Hong Kong, especially with over 90% of commercial buildings in Hong Kong equipped with the MVAC system.[2] Such emissions from an MVAC system may create an impact for infection control in offices.

This study evaluates the exposure concentration of the bioaerosol emission from MVAC systems to the building occupants. The exposure level for building occupants had been investigated under the influence of the bioaerosol emission and ventilation rate (VR), in terms of air change rate per hour (ACH). A two-phase flow computational fluid dynamics (CFD) simulation of a typical office cubicle of Hong Kong was conducted by ANSYS Fluent (i.e. Version 14) with various bioaerosol emission concentrations, VRs, and microorganism species. The findings can be used by the building management to minimize bioaerosol exposure for maintenance strategies of MVAC systems.

Two-phase flow CFD models for bioaerosol particle simulation

Bioaerosol particles in the indoor air are related to spreading of airborne infectious diseases and some pandemic outbreaks such as Severe Acute Respiratory Syndrome (SARS) in 2003 and Middle East Respiratory Syndrome (MERS) in 2015. Several environmental control strategies and parameters for a ventilation system have been suggested to prevent infections in building environments.[9] To design an appropriate ventilation system, some infection risk models were proposed in order to achieve effective infection control such as Wells–Riley and dose–response.[10] CFD simulation is often used to predict the spatial and temporal distributions of bioaerosol particles for the infection risk assessment for indoor airflow (i.e. $Re_{bp} < 1$).[11]

For bioaerosol particle movement simulation, the drift-flux model (DFM) and discrete phase model (DPM) are two commonly used approaches in gas–particle flow CFD simulation.[12] Since the size of the bioaerosol particles is less than 100 μm, it was assumed to be airborne,[13] and the gas–gas two-phase CFD simulation has been used to estimate bioaerosol particle dispersion by a DFM under a Eulerian–Eulerian framework.[14] However, the behavior of bioaerosol particles in air differ from that of gas molecules for the same boundary condition. For example, bioaerosol particles maintain higher momentum (i.e. velocity) along with an airstream when compared with the rapid momentum decay of gas molecules.[15]

In addition, the molecular diffusion could be neglected for bioaerosol.[15–17] DPM has been proposed to predict bioaerosol particle movement by the force balance of the interactions with the continuum phase in equation (1). This Maxey and Riley equation is derived from the Basset–Boussinesq–Oseen equation without the Faxen term due to the curvature of the velocity field.[15,18,19]

$$F_{bp} = F_{drag} + F_{grav} + F_{SL} + F_{Brown} \tag{1}$$

where F_{bp} is the force acting on a bioaerosol particle (N), F_{drag} is the drag force (N), F_{grav} is the gravity force, and F_{SL} is Saffman's lift force for an inviscid fluid.[20,21] F_{Brown} is the Brownian force for submicron bioaerosol particle.[22] In addition, the Cunningham slip correction factor f_{slip} was also recommended in drag force F_{drag} in the submicron range in equation (2).[23]

$$F_{drag} = m_{bp} \times f_{slip} \frac{18\mu_{air} C_{drag} \mathrm{Re}_{bp}}{24\rho_{bp} d_{bp}^2} \left(v_{air} - v_{bp}\right) \tag{2}$$

where m_{bp} is the mass of the bioaerosol particle, C_{drag} is the drag coefficient, d_{bp} is the diameter of the bioaerosol particle, v_{bp} and v_{air} are the velocities of the bioaerosol particle and air ($\mathrm{m\,s^{-1}}$), respectively, ρ_{bp} is the bioaerosol particle density ($\mathrm{kg\,m^{-3}}$), ρ_{air} is the air density ($\mathrm{kg\,m^{-3}}$), μ_{air} is the molecular viscosity of air ($\mathrm{kg\,m^{-1}\,s^{-1}}$), and Re_{bp} is the Reynolds number for bioaerosols in an airflow field below[24]

$$\mathrm{Re}_{bp} = \frac{\rho_{air} d_{bp} \left| v_{air} - v_{bp} \right|}{\mu_{air}} \tag{3}$$

These equations demonstrated that the Eulerian–Lagrangian framework provides an accurate prediction of the turbulent transport of discrete particles by comparison with direct numerical simulation results and the widely referred wind-tunnel experiments.[25] Stochastic fluctuations are complemented with statistical turbulent dispersions by discrete random walk, although the instantaneous turbulence quantities of the dispersed phase cannot be solved by the Reynolds-averaged Navier–Stokes (RANS) model.[15]

In addition, the drag coefficient and the drag constant of bioaerosol particle are suggested to relate its equivalent bioaerosol diameter d_{ebd} as particle diameter in terms of its shape, surface texture, and elasticity which are different from the aerosol particle in equation (4)[26]

$$C_{drag} = \frac{K_{drag}}{\mathrm{Re}_{bp}} \quad \mathrm{Re}_{bp} < 1 \tag{4}$$

and equation(5)

$$K_{drag} = \frac{d_{ebd}^2}{2} \quad 0.69\,\mu\mathrm{m} \le d_{ebd} \le 6.9\,\mu\mathrm{m};\ 1 \le r_{aspect} \le 6.9 \tag{5}$$

Using equations (6) and (7), the equivalent bioaerosol diameter d_{ebd} and aspect ratio can be determined from electron micrographs by the projected image area, length, and width which are A_b, l_1, and l_2, respectively.[27,28]

$$d_{ebd} = 2\sqrt{\frac{A_{proj}}{\pi}} \tag{6}$$

$$r_{aspect} = \frac{\max(l_1, l_2)}{\min(l_1, l_2)} \tag{7}$$

This model provides a simple and quick tool to simulate the dispersion and deposition of the bioaerosol particles in two-phase flow CFD simulation. The model also suggests a numerical method to understand the spreading process of airborne infectious disease and evaluate the exposure risk assessment for infection control application in workplace environments.

CFD simulation for bioaerosol exposure for a workplace environment

Application of health risk assessment for an office cubicle

In this section, a continuous emission from the MVAC system was suggested to simulate the bioaerosol exposure level in an office cubicle. A numerical bioaerosol transport framework in Figure 1, which is based on the empirical bioaerosol drag coefficient model.[26] It was adopted to simulate the emission, dispersion, deposition, and exhaustion of bioaerosol particles from the MVAC systems in a typical office room (i.e. Office A) by altering the ventilation strategies with four VRs, four emission concentrations, and two microorganism species. The findings of the simulation

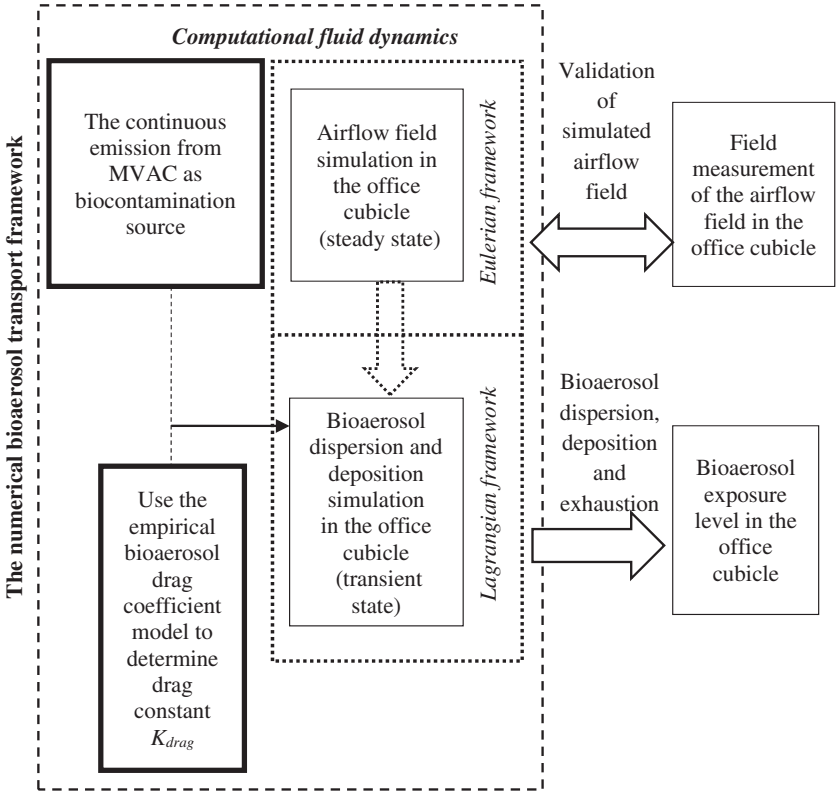

Figure 1. The numerical bioaerosol particle transport framework for the office cubicle simulation.
MVAC: mechanical ventilation and air conditioning.

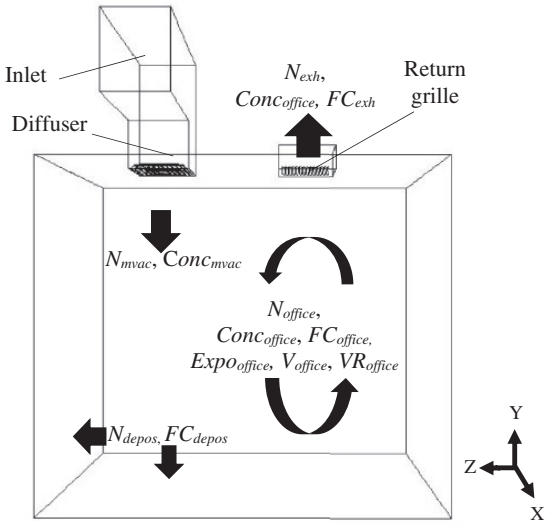

Figure 2. Typical mixing ventilation for an office.

provided the bioaerosol concentration and exposure levels by bioaerosol emission from an MVAC system. This simulation also suggested the building management to plan the maintenance strategies of the MVAC systems for minimizing bioaerosol exposures in offices.

Determination of exposure level from a continuous emission source

Exposure to over a period of time can be represented by a time-variant bioaerosol exposure concentration in concentration–time units in equation (8).

$$Expo_{office} = \int Conc_{office}(t)\mathrm{d}t \tag{8}$$

where $Expo_{office}$ is the exposure level of an office (CFU min m^{-3}), $Conc_{office}(t)$ is the exposure concentration (CFU m^{-3}) as a function of time t (min).[29]

Figure 2 illustrates the typical mixing ventilation of an MVAC system for an office. By mass conservation, the change of bioaerosol particles in the office with time must be equal to the difference between the bioaerosol sources (i.e. from the MVAC system only, no other bioaerosol emission source was assumed inside the office) and sinks (i.e. exhaust to the MVAC and deposition on room surfaces) for a single-zone ventilation model. The concentration (CFU m^{-3}) could be estimated by particle counts and office cubicle volume in equation (9).

$$Conc_{office} = \frac{N_{office}}{V_{office}} \tag{9}$$

where N_{office} is the number of bioaerosol particles suspended in the office and V_{office} is the office cubicle volume (m^3). For each bioaerosol species, same bioaerosol particle masses are supposed for monodisperse equivalent bioaerosol diameter d_{ebd}.[30] The N_{office} could be derived to equation (10) in the form of a bioaerosol particle count for continuous emission.[31]

$$N_{office} = \sum N_{mvac} - \sum N_{exh} - \sum N_{depos} \tag{10}$$

Bioaerosol particles suspended in the office N_{office} is equal to the bioaerosol particles generated from an MVAC system N_{mvac} (in counts) removed by the exhaust N_{exh} and deposited on room surfaces N_{depos} without resuspension. The growth and death of the microorganisms were ignored due to the simulation focused on the contribution of the continuous bioaerosol emission from ventilation system and only lasted for 1 h.

The bioaerosol emission concentration from an MVAC system $Conc_{mvac}$ is varied by the MVAC system configuration such as a ratio of fresh air and recirculation air or an outdoor bioaerosol concentration. In this simulation, the bioaerosol concentrations before diffusers and VR were used as the final outcomes from the MVAC system. These variables could be estimated from bioaerosol particle movements by CFD simulations. To understand the bioaerosol removal process, the bioaerosol fractional counts FC_{office}, FC_{exh}, and FC_{depos} are given below in equation (11).

$$FC_{office} = \frac{N_{office}}{\sum N_{mvac}}; \quad FC_{exh} = \frac{N_{exh}}{\sum N_{mvac}}; \quad FC_{depos} = \frac{N_{depos}}{\sum N_{mvac}} \tag{11}$$

By combining equations (9) and (10), the accumulated emitted number of the particles is equal to the sum of FC_{office} and accumulated FC_{exh} and FC_{depos} due to the continuous injection of the bioaerosol particles from the MVAC system in equation (12).

$$\sum FC_{mvac} = FC_{office} + \sum FC_{exh} + \sum FC_{depos} \tag{12}$$

To confirm the mass balance between the bioaerosol emission and the sum of the exhaust, deposition, and suspension, Figure 3 provides a visual integration of these fractional counts FC_{office}, FC_{exh}, FC_{depo}, and FC_{mvac} in equation (12) for the two-phase CFD simulation.

The proposed transport simulation framework provides a tool to evaluate the exposure level of the office environment that bioaerosols emitted from MVAC systems or other continuous emission sources. For the

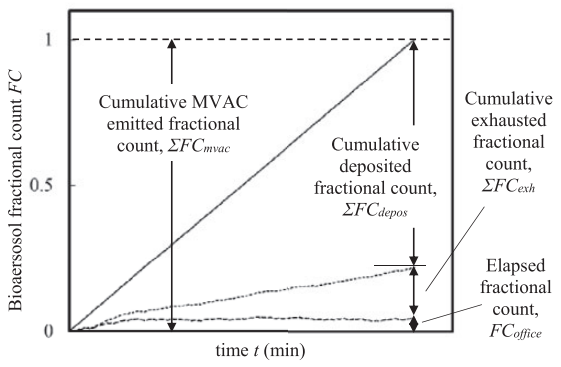

Figure 3. Description of the bioaerosol removal process. MVAC: mechanical ventilation and air conditioning.

continuous bioaerosol, a Scheme script, which is an automation script for Fluent, was written to implement the dynamic source emission by time interval injection in Table 1.

Numerical simulations of bioaerosol exposure level of an office cubicle of Hong Kong

Four common indoor VRs VR_{office} (i.e. 1, 5, 9, and 13 ACHs), four bioaerosol emission concentrations from the MVAC system $Conc_{mvac}$ (i.e. $Conc_{mvac} = 100$, 200, 300, and 400 CFU m^{-3}), and two emission microorganism species (i.e. *Cladosporium cladosporioides* (ATCC16021) and *Staphylococcus aureus* (ATCC

Table 1. Fluent Scheme program for the continuous emission source.

```
;; ****************************************************************
;; Scheme program for a continuous emission source for an hour
;; by John Yu, Ho Ching on 25 Dec 2015
;; ****************************************************************
(define den 1100);; density
(define dia 0.69);; particle diameter in (um)
(define conc 100);; bioaerosol emission concentration (CFU m-3)
(define num_pat (* 35.991 ach conc));; calculate no of particles in hr by RmVol in m3
(define time_pat (/3600 num_pat));; calculate the time between each particle
;; ************************************************
;; function to run the 3 simulation in same configuration to average
;; ************************************************
(define (sample_udf_run dia vel den num_pat shape_fac c1 c2 c3 loop)
        ;; Getting the variable from UDF file
        (if (not (rp-var-object 'cd_eqt/c1))
           (rp-var-define 'cd_eqt/c1 0 'real #f))
        (if (not (rp-var-object 'cd_eqt/c2))
           (rp-var-define 'cd_eqt/c2 0 'real #f))
        (if (not (rp-var-object 'cd_eqt/c3))
           (rp-var-define 'cd_eqt/c3 0 'real #f))
        ;; Set density
        (format "\n set density")
        (ti-menu-load-string
              (format #f " define/materials/change-create/anthracite anthracite y ~a n n " den)
        )
        ;; set max-step
        (format "\n set max-step")
        (ti-menu-load-string
              " define/models/dpm/numerics/tracking-parameters 500000 n 5"
        )
        ;; set diameter and number of particles
        (format "\n set injection")
        (ti-menu-load-string
           (format #f
           "define/injections/set-injection-properties
           injection-0 injection-0 n n n inlet inlet () n n y n ~a 0.15000001 n n n n 0 0 0 ~a 0" num_pat (* dia 1e-06)
              )
        )
        ;; set the drag parameter
```

(continued)

Table 1. Continued

```
        ;;(format "\n cd_eqt/c1 ~a =" cd_eqt/c1)
        (format "\n set drag parameter")
        (ti-menu-load-string
        " define/models/dpm/numerics/drag-law particle_drag_force_count::libudf "
        )
        ;; Run the simulation with a continuous emission source
        (format "\n set emission rate = ~a" time_pat)
        (ti-menu-load-string
          (format #f " define/models/dpm/unsteady-tracking yes no ~a yes " time_pat)
        )
        ;; Run the simulation at different elapse time
        (do ((j 1) (i 1 (+ i 1))) ((> i 36000) j);; an hour
          (ti-menu-load-string (format #f "solve/dual-time-iterate 1 1"))
          (format "\n injection \n")
          (ti-menu-load-string
                (format #f
                  "define/injections/set-injection-properties injection-0 injection-0 n n n n n n n 2.15 3.5 2.35 0 0 0 ~a 300 0 ~a ~a
" (* dia 1e-06) 0 10000
          )
        )
        ;;;; run the particles track
        (ti-menu-load-string (format #f "display/set/particle-tracks/report-type summary "))
        (ti-menu-load-string (format #f "display/set/particle-tracks/history-filename \"summary_~a_ach_~a_conc_~a_dia_~a_elap
sed_~a_time_~a.dpm\" " bn ach conc dia elapsed_time i))
          (format "\n Tracking...")
          (ti-menu-load-string (format #f "display/particle-tracks/particle-tracks particle-id injection-0 () 0 0 "))
        )
)
;; ***************************************************************
;; main program for running the batch
;; ***************************************************************
{
          (format "\n Program Start")
          (define c1 0)
          (define c2 0.23805)
          (define c3 0)
          ;; generator fluent default
          ;;(sample_fluent_run dia vel den num_pat 1 0 24 0 loop)
          (do ((s 0) (t 1 (+ t 1))) ((= t 2) s)
          (do ((l 0) (k 1 (+ k 1))) ((= k 2) l)
          ;; case k for k1 of drag constant
            (format "\n C2 == ~a " c2)
            ;; calling the sub program in run CFD simulation
            (format "\n conc of bacteria emission on ~d step - STARTED " conc)   (sample_udf_run dia vel den conc 1 c1 c2 c3 t)
          )
)
```

6538)) were used to demonstrate the effect of the bioaerosol exposure concentration of building occupants by the bioaerosol emission from an MVAC system in a typical small office cubicle (i.e. Office A) of Hong Kong. Both *C. cladosporioides* and *S. aureus* are the commonly found bacterial and fungal genera in ventilated buildings with relative abundance of up to 100% in the air samples as illustrated in Figure 4.[8] Their equivalent bioaerosol diameters d_{ebd} and drag constants K_{drag} are summarized in Table 2.

Office A with dimensions of 4.3 m (L) × 3.1 m (W) × 2.7 m (H) is illustrated in Figure 5. There was an air inlet with a ceiling-mounted diffuser in the cubicle and a return grille as an air outlet. The bioaerosol particles were continuously emitted 0.5 m above the diffuser. The distance provided the bioaerosol particles to

Table 2. Information of the bioaerosol species.

Species	ATCC	Relative abundance	Equivalent bioaerosol diameter d_{ebd} (μm)[a]	Aspect ratio r_{aspect}	Drag constant K_{drag}
Staphylococcus aureus	ATCC 6538	5 ~ 10%	0.69 ± 0.02	1.0	0.23805
Cladosporium cladosporioides	16021	17 ~ 22%	3.4 ± 0.09	2.1	5.78

[a]Standard errors are shown.

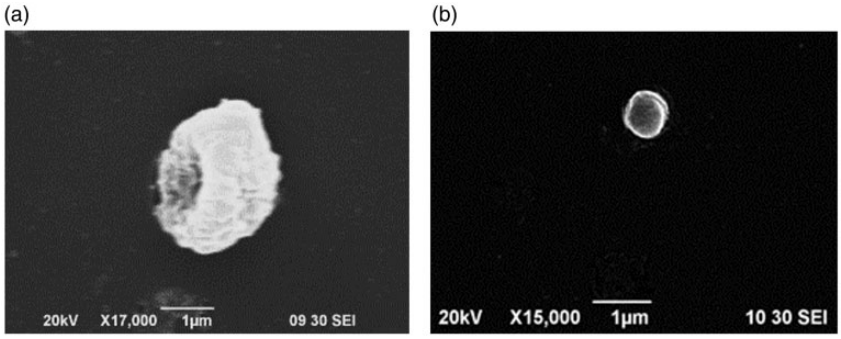

Figure 4. Referenced SEM photos of the bioaerosol species. (a) *Cladosporium cladosporioides* (ATCC16021), (b) *Staphylococcus aureus* (ATCC 6538).

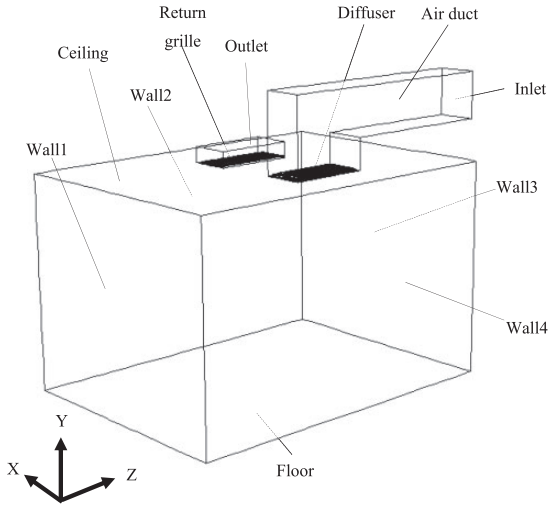

Figure 5. The layout and CFD configurations in Office A.

be initial as if the particles emitted from the MVAC system in terms of velocity and distribution before the diffuser. The particle injection time was calculated from the emission concentration $Conc_{mvac}$ and VR VR_{office}. After the injection, the positions and velocities of the bioaerosol particles were updated by DPM until deposited on the walls of the office or discharged to the outlet. The walls of the office were insulated well and considered to be adiabatic. The room temperature was assumed to be 22.9°C, which is the average temperature from a survey of 2133 air-conditioned office buildings of Hong Kong.[32]

The airflow simulation results were compared with onsite measurements of air velocity v_{air} (by Dantec Dynamic ComfortSense and 54T33 omnidirectional velocity probes) at the VR_{office} (by Shortridge FlowHood ADM-870C) of 2.1 ACH in the office. No significant difference was reported between measurement and simulation for Office A ($n = 58$, $p > 0.9$, t test). The simulation settings and boundary conditions inside the office cubicle are summarized in Table 3.

Results of the bioaerosol exposure in the office cubicle of Hong Kong

Effect of the continuous emission from the MVAC system in an office cubicle

Figure 6 shows the dynamic bioaerosol concentration in the office cubicle $Conc_{office}$ within an hour with various *S. aureus* emission concentration $Conc_{mvac}$ (i.e. 100, 200, 300, and 400 CFU m^{-3}) and VR_{office} (i.e. 1, 5, 9, and 13 ACH) from the MVAC system. Generally, the bioaerosol concentration became steady in condition within first 10 min. The steady concentration levels $Conc_{office}$ were found similar at the same emission concentrations $Conc_{mvac}$, even at different VRs. For example, around 5 CFU m^{-3} of steady concentration levels $Conc_{office}$ were observed in all 100 CFU m^{-3} emission concentration $Conc_{mvac}$ with the four VR_{office} (i.e. 1, 5, 9, and 13 ACH). Around 5% of the emission concentration from the MVAC system $Conc_{mvac}$ contributes to

Table 3. CFD simulation settings and boundary conditions.

Computational domain	4.3 m (L) × 3.1 m (W) × 2.7 m (H)
Solver	DPM, RANS, RNG k-ε turbulence model, PISO, SIMLPE, standard wall function
Mesh configuration	1466K cells, $f_{asymp} = 0.997$, $GCI_{coarse} = 29\%$ and $GCI_{fine} = 62\%$
Total supply airflow rate	0.12 kg s^{-1} (for $VR_{office} = 1$ ACH), 0.61 kg s^{-1} (for $VR_{office} = 5$ ACH), 1.1 kg s^{-1} (for $VR_{office} = 9$ ACH), and 1.59 kg s^{-1} (for $VR_{office} = 13$ ACH), 22.9°C (air temperature)
Diffuser (0.5 m × 1 m)	Four-way spread-type, supply jets had an angle of 15° from ceiling, adiabatic, and reflect boundary type
Return grille (0.5 m × 1 m)	Pressure-outlet, 22.9°C (backflow temperature), adiabatic, escape boundary type
Walls, ceiling, floor and beds	No slip wall boundary, 22.9°C (surface temperature), adiabatic, trap boundary type
Bioaerosol emission source	Continuous-shot release from the diffuser, density of bioaerosol particle $\rho_{bp} = 1100$ kg m^{-3}, initial velocity $v_{bp} = 0$ m s^{-1}, equivalent bioaerosol diameter $d_{ebd} = 0.69$ μm (for *Staphylococcus aureus*) and 3.4 μm (for *Cladosporium cladosporioides*), total emission particles in an hour N_{mvac}: 3600 (for $Conc_{mvac} = 100$ CFU m^{-3}), 7200 (for $Conc_{mvac} = 200$ CFU m^{-3}), 10800 (for $Conc_{mvac} = 300$ CFU m^{-3}), and 14,400 (for $Conc_{mvac} = 400$ CFU m^{-3}).

CFD: computational fluid dynamics.

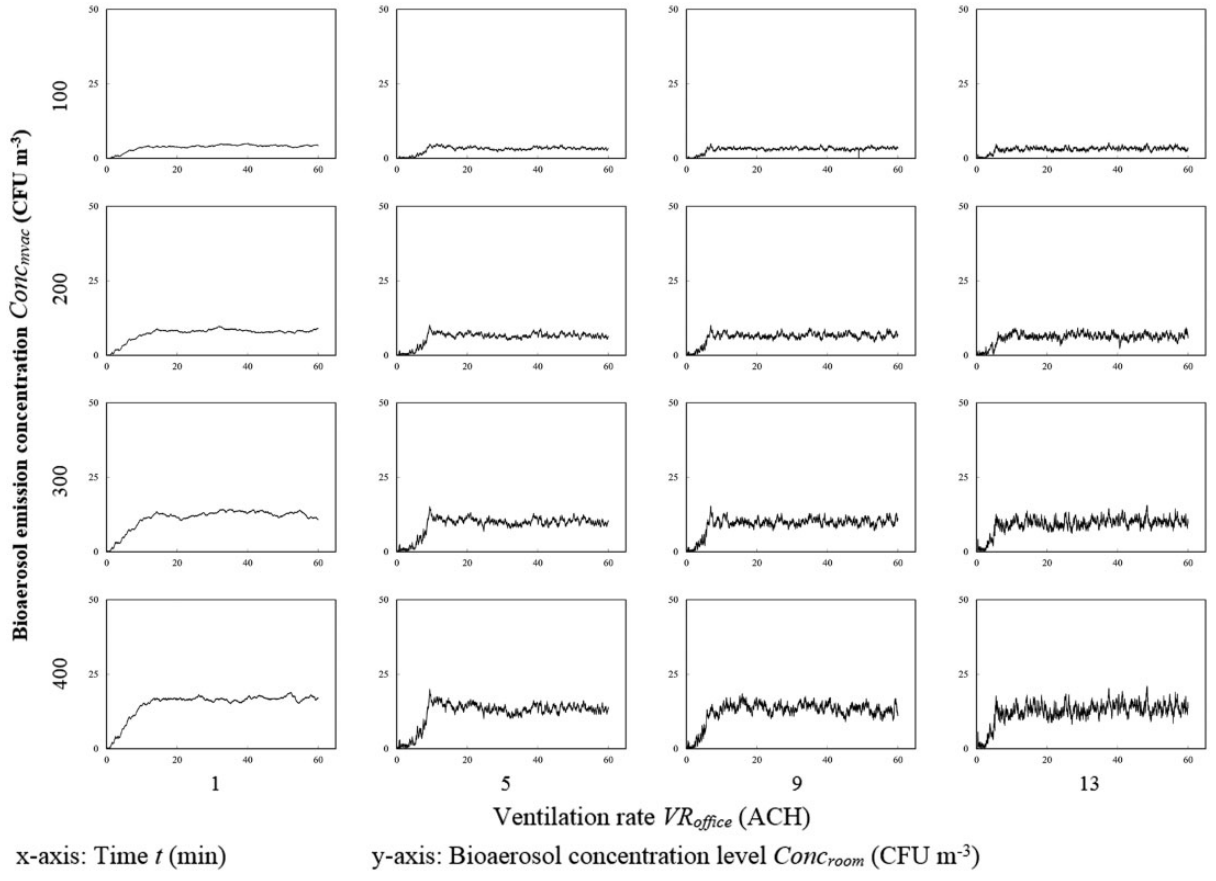

Figure 6. *Staphylococcus aureus* concentration level for ventilation rates and emission concentrations.
ACH: air change rate per hour; CFU: colony-forming unit.

the bioaerosol concentration inside the cubicle. The VR_{office} seem less sensitive to the bioaerosol concentration level in room $Conc_{office}$ instead of the bioaerosol emission concentration $Conc_{mvac}$. Only the high fluctuation of the bioaerosol concentrations in room $Conc_{office}$ was associated with the high VR_{office} (i.e. 9 and 13 ACH) that demonstrates the dynamic equilibrium on the steady concentration levels.

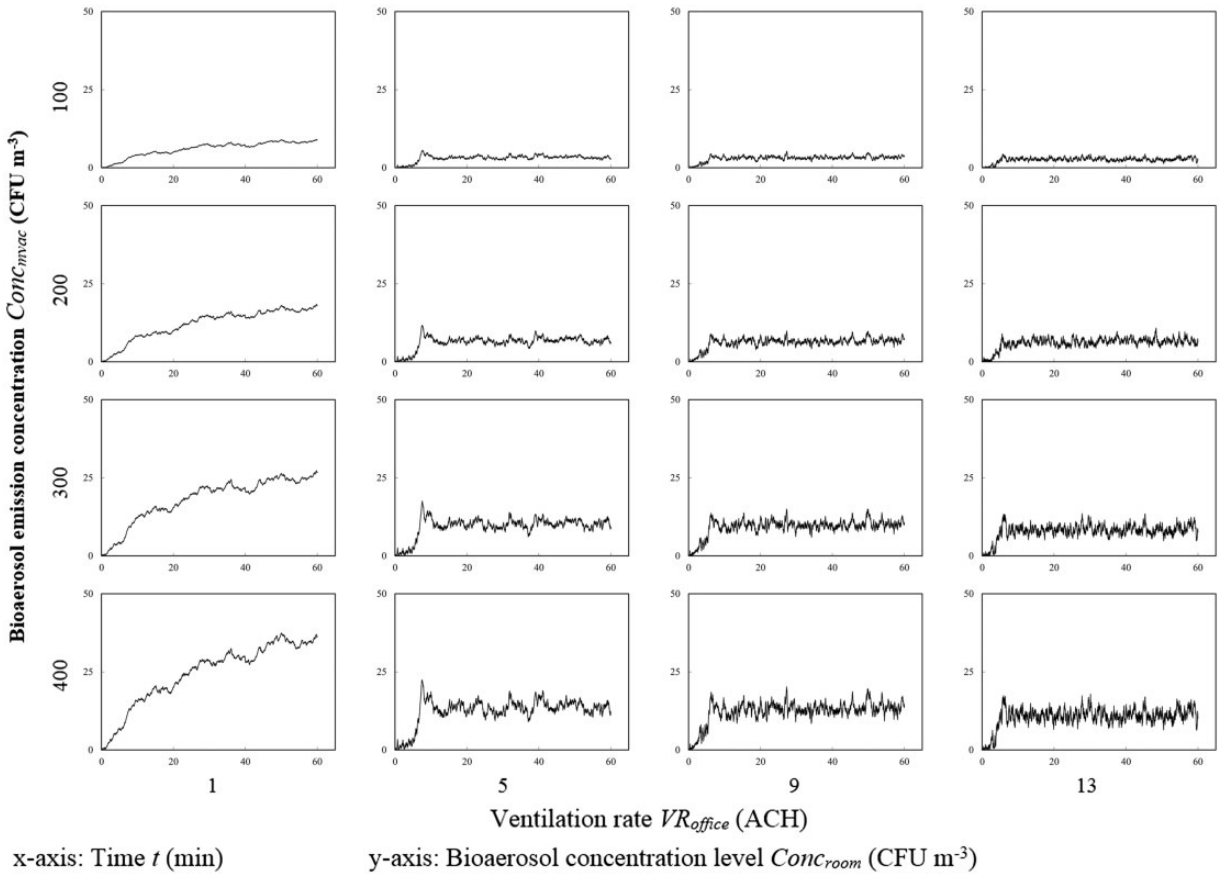

Figure 7. *Cladosporium cladosporioides* concentration level for ventilation rates and emission concentrations. ACH: air change rate per hour; CFU: colony-forming unit.

In Figure 7, the similar results of *C. cladosporioides* were found, except VR_{office} at 1 ACH. The non-steady state conditions of the *C. cladosporioides* concentration level indicate the VR_{office} (i.e. 1 ACH) was insufficient to balance the concentration level to the equilibrium state. The VR was not enough to dilute the larger bioaerosol particles (3.4 μm) in Office A since the higher gravity force and inertia are proportional to the particle mass (i.e. d_{ebd}^3).[26]

The insufficient VR_{office} (i.e. 1 ACH) of *C. cladosporioides* and *S. aureus* were also demonstrated in the bioaerosol fractional count *FC* in Figure 8. Larger elapsed fractional counts FC_{depos} of *C. cladosporioides* and *S. aureus* were found at 1 ACH of VR_{office} by comparing with other VRs. In addition, the elapsed fractional counts FC_{office} doubled between *S. aureus* and *C. cladosporioides*. Due to *C. cladosporioides* particles were accumulated in Office A in a higher number and stayed longer than *S. aureus* particles. The maximum elapsed time t_{max_office} of *C. cladosporioides* (i.e. 14 min) was almost twice than that of *S. aureus* (i.e. 7 min) by a single-shot of 11,500 bioaerosol particles emission in Figure 9. Both findings reported that the insufficient VRs VR_{office} leads to non-steady concentration levels $Conc_{office}$ and larger elapse fraction counts FC_{depos} from the MVAC system.

Large deposited fractional count FC_{depos} (i.e. >0.8) also shows the large portions of bioaerosol particles deposited in the office surfaces (i.e. Wall2, Wall3, and Wall4) instead of those exhausted to the return grille (i.e. outlet) in Figure 8. These depositions may cause high infection risk via surface contact. For bacterial species, *S. aureus* are expected to decay in air and office surfaces in the office environments. However, *C. cladosporioides* may grow to form mould on the office's walls or ceilings as fungal species.

Exposure level with the bioaerosol emission concentration from the MVAC system

The correlation of the bioaerosol exposure level $Expo_{office}$ and emission concentration from the MVAC system is indicated in Figure 10. Linear correlations of all the VRs were reported. The exposure levels of the non-steady states (i.e. 1 ACH of VR_{office} for

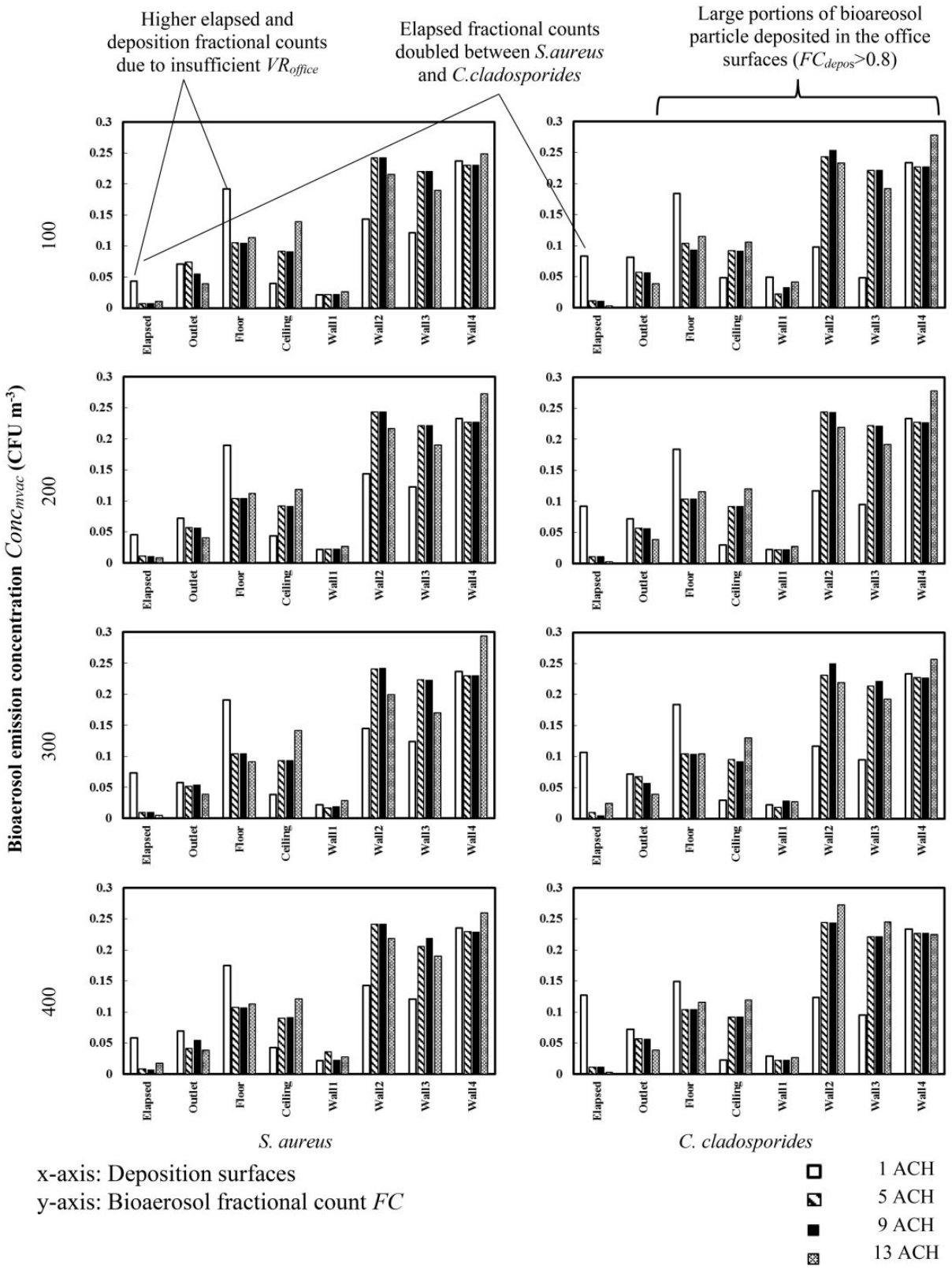

Figure 8. Fractional count of bioaerosol particles for concentration distributions and deposition patterns for *S. aureus* and *C. cladosporioides*.

ACH: air change rate per hour; CFU: colony-forming unit.

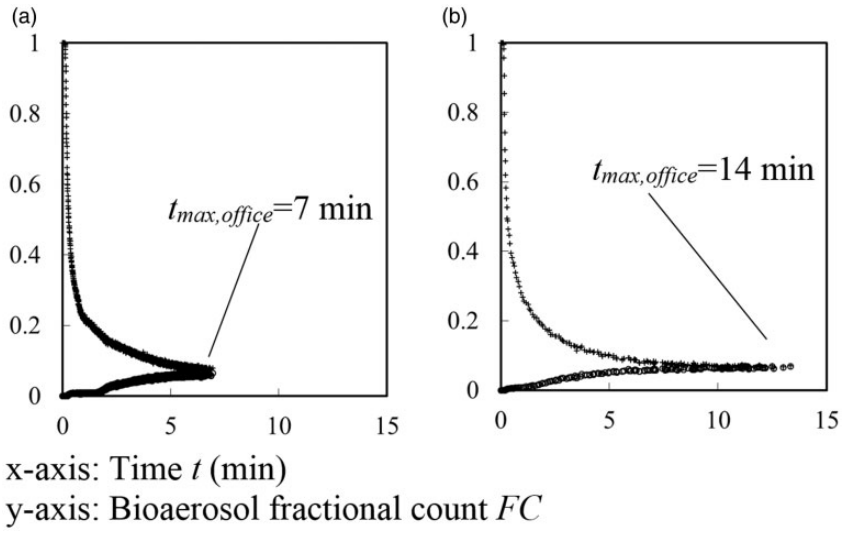

Figure 9. Fractional count of bioaerosol particles for single-shot emission at 1 ACH of VR_{office}. (a) *S. aureus* and (b) *C. cladosporioides*.

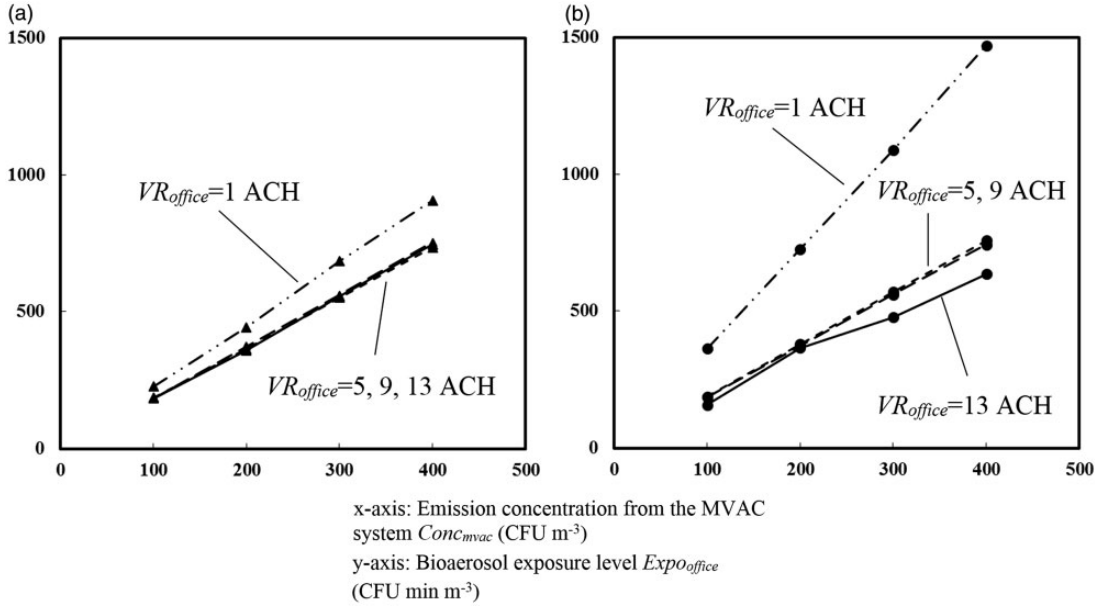

Figure 10. Bioaerosol exposure level with different emission concentrations. (a) *S. aureus* and (b) *C. cladosporioides*. ACH: air change rate per hour; CFU: colony-forming unit; MVAC: mechanical ventilation and air conditioning.

C. cladosporioides) are doubled from the steady state conditions of concentration levels that suggested the sufficient level of the VR that can contribute to dilute the bioaerosol particles in the room. There is a great difference when the VR is insufficient to achieve the steady state conditions of concentration level and reduce the exposure level. The critical VR is varied with the bioaerosol species in terms of the equivalent bioaerosol diameter d_{ebd}; however, the value should be the minimum requirement for the MVAC system to avoid the accumulation of bioaerosol particles and infection risk. Over this critical VR, the exposure level has only 5% contribution from the emission concentration from the MVAC system.

The findings remind us of the importance of maintaining the cleanliness of the ventilation system (i.e. filter cleaning) instead of just considering the ventilation system design process or infection control. In addition, the installation of ultraviolet germicidal irradiation devices inside the MVAC system is also recommended for the disinfection of microorganisms. The provision of the fresh air could also help to dilute the

emission concentration by mixing with the recirculation air. However, the VR is not associated with the recirculation ratio of the ventilation system instead of airflow dominated. The balance of infection control and energy efficiency have to be further investigated. The two-phase flow CFD application for bioaerosol particle simulated an exposure risk assessment of the office cubicle with ventilation system parameters in terms of VR, emission concentration, and emission species. The results provide the useful information to the building management to minimize bioaerosol exposure for maintenance strategies of an MVAC system for public health.

Conclusion

The study indicates the bioaerosol emission concentration is a major factor for the concentration and exposure level in an office environment. The cleanliness and maintenance of an MVAC system are important to reduce the bioaerosol emission from an MVAC system. In addition, UVGI lamps are recommended to install inside MVAC systems for microorganisms disinfection. For VR, it is critical to maintain a steady state of concentration level. The bioaerosol emission concentration level contributes only 5% to the concentration level in an office environment if the VR is sufficient to balance the emission. However, the balance of infection control and energy efficiency could be further investigated on the recirculation ratio of the ventilation system instead of fresh air. The two-phase flow simulation provides an exposure risk assessment application to study the interaction between the bioaerosol particle and airflow inside a typical Hong Kong office environment.

Declaration of conflicting interests

The author(s) declared no potential conflicts of interest with respect to the research, authorship, and/or publication of this article.

Funding

The author(s) disclosed receipt of the following financial support for the research, authorship, and/or publication of this article: The work described in this paper was partially supported by the grants from The Hong Kong Polytechnic University (Project account number G-YBA7).

References

1. Douwes J, Thorne P, Pearce N, et al. Bioaerosol health effects and exposure assessment: progress and prospects. *Ann Occup Hyg* 2003; 47: 187–200.
2. Chow PW, Chan WY and Vrijmoed LLP. An investigation on the occurrence of fungi and bacteria in the MVAC system in an office premise. In: *Proceedings of the 10th international conference on indoor air quality and climate "Indoor Air 2005,"* Beijing, China, 4–9 September 2005.
3. Bluyssen PM, Cox C, Seppänen O, et al. Why, when and how do HVAC-systems pollute the indoor environment and what to do about it? The European AIRLESS project. *Build Environ* 2003; 38: 209–225.
4. Zuraimi MS. Is ventilation duct cleaning useful? A review of the scientific evidence. *Indoor Air* 2010; 20: 445–457.
5. Hugenholtz P and Fuerst JA. Heterotrophic bacteria in an air-handling system. *Appl Environ Microbiol* 1992; 58: 3914–3920.
6. Schmidt MG, Attaway HH, Terzieva S, et al. Characterization and control of the microbial community affiliated with copper or aluminum heat exchangers of HVAC systems. *Curr Microbiol* 2012; 65: 141–149.
7. Wu PC, Li YY, Chiang CM, et al. Changing microbial concentrations are associated with ventilation performance in Taiwan's air-conditioned office buildings. *Indoor Air* 2005; 15: 19–26.
8. Meadow JF, Altrichter AE, Kembel SW, et al. Indoor airborne bacterial communities are influenced by ventilation, occupancy, and outdoor air source. *Indoor Air* 2014; 24: 41–48.
9. Sundell J, Levin H, Nazaroff WW, et al. Ventilation rates and health: multidisciplinary review of the scientific literature. *Indoor Air* 2011; 21: 191–204.
10. Sze To GN and Chao CYH. Review and comparison between the Wells-Riley and dose-response approaches to risk assessment of infectious respiratory diseases. *Indoor Air* 2010; 20: 2–16.
11. Sze To GN, Wan MP, Chao CY, et al. A methodology for estimating airborne virus exposures in indoor environments using the spatial distribution of expiratory aerosols and virus viability characteristics. *Indoor Air* 2008; 18: 425–438.
12. Holmberg S and Li Y. Modelling of the indoor environment – particle dispersion and deposition. *Indoor Air* 1998; 8: 113–122.
13. Wells WF. On air-borne infection: study II. Droplets and droplet nuclei. *Am J Epidemiol* 1934; 20: 611–618.
14. Hibiki T and Ishii M. One-dimensional drift-flux model and constitutive equations for relative motion between phases in various two-phase flow regimes. *Int J Heat Mass Transfer* 2003; 46: 4935–4948.
15. Wan MP. *Indoor transport of human expiratory droplets in association with airborne infectious disease transmission using a multiphase-flow approach*. HKSAR, China: The Hong Kong University of Science and Technology, 2006.
16. Pantelic J, Sze-To GN, Tham KW, et al. Personalized ventilation as a control measure for airborne transmissible disease spread. *J R Soc Interface* 2009; 6: S715–S726.
17. Nicas M, Nazaroff WW and Alan H. Toward understanding the risk of secondary airborne infection: emission of respirable pathogens. *J Occup Environ Hyg* 2005; 2: 143–154.
18. Oseen CW. *Neuere Methoden und Ergebnisse in der Hydrodynamik*. Leipzig: Akademische Verlagsgesellschaft m. b. h., 1927.

19. Basset AB. *A treatise on hydrodynamics, with numerous examples*. London, UK: Cambridge Deighton, Bell and Co., 1888.
20. Saffman PG. The lift on a small sphere in a slow shear flow. *J Fluid Mech* 1965; 22: 385–400.
21. Lai ACK, Wong LT, Mui KW, et al. An experimental study of bioaerosol (1-10um) deposition in a ventilated chamber. *Build Environ* 2012; 56: 118–126.
22. Morawska L. Droplet fate in indoor environments, or can we prevent the spread of infection? *Indoor Air* 2006; 16: 335–347.
23. Chao CYH and Wan MP. A study of the dispersion of expiratory aerosols in unidirectional downward and ceiling-return type airflows using a multiphase approach. *Indoor Air* 2006; 16: 296–312.
24. ANSYS. *ANSYS fluent theory guide 14.0*. Canonsburg, PA: ANSYS Inc., 2011.
25. Snyder WH and Lumley JL. Some measurements of particle velocity autocorrelation functions in a turbulent flow. *J Fluid Mech* 1971; 48: 41–71.
26. Wong LT, Yu HC, Mui KW, et al. Drag constants of common indoor bioaerosols. *Indoor Built Environ* 2015; 24: 401–413.
27. Ferreira T and Rasband W. ImageJ user guide/Fiji 1.46, 2012.
28. Wagner J and Macher J. Automated spore measurements using microscopy, image analysis, and peak recognition of near-monodisperse aerosols. *Aerosol Sci Tech* 2012; 46: 862–873.
29. USEPA. *Air quality criteria for particulate matter* (*final report, Oct 2004*). Contract No. EPA 600/P-99/002aF-bF, 2004. Washington, DC: US Environmental Protection Agency.
30. Kim D-j, Chung S-g, Lee S-h, et al. Relation of microbial biomass to counting units for *Pseudomonas aeruginosa*. *Afr J Microbiol Res* 2012; 6: 4620–4622.
31. Toivola M, Nevalainen A and Alm S. Personal exposures to particles and microbes in relation to microenvironmental concentrations. *Indoor Air* 2004; 14: 351–359.
32. Mui KW, Wong LT, Xiao F, et al. Development of sustainable building environmental model (SBEM) in Hong Kong. In: *ICEEE 2015: 17th international conference on energy and environmental engineering*, London, United Kingdom, 25–26 July 2015.

Appendix 1

Notation

A	area (μm^2)
A_{proj}	projected image area of a particle (μm^2)
C_{drag}	drag coefficient
$Conc_{mvac}$	concentration level emitted from the MVAC system (CFU m^{-3})
$Conc_{office}$	concentration level in the office cubicle (CFU m^{-3})
d_{bp}	bioaerosol particle diameter (μm)
d_{ebd}	equivalent bioaerosol diameter (μm)
$Expo_{office}$	exposure level (CFU min L^{-1})
f_{asymp}	asymptotic range of convergence
f_{slip}	cunningham slip correction factor
F_{bp}	force acted on a bioaerosol particle (N)
F_{Brown}	Brownian force (N)
F_{drag}	drag force (N)
F_{grav}	gravity force (N)
F_{SL}	Saffman's lift force (N)
FC_{depos}	fractional count of bioaerosol particles deposited onto surfaces
FC_{exh}	fractional count of bioaerosol particles removed through exhaust
FC_{office}	fractional count of bioaerosol particles elapsed in the office
GCI	grid convergence index
K_{drag}	drag constant
l_1	length of a bioaerosol particle (μm)
l_2	width of a bioaerosol particle (μm)
m_{bp}	mass of a bioaerosol particle (kg, g)
N_{depos}	number of bioaerosol particles deposited onto surfaces
N_{exh}	number of bioaerosol particles removed through exhaust
N_{mvac}	number of bioaerosol particles from MVAC system
N_{office}	number of bioaerosol particles elapsed in the office
p	p value
r_{aspect}	aspect ratio of bioaerosol particles
Re_{bp}	Reynolds number for bioaerosol particles
t	time (min)
t_{max_office}	maximum elapsed time (min)
v_{air}	air velocity (m s^{-1})
v_{bp}	bioaerosol particle velocity (m s^{-1})
V_{office}	volume of office cubicle (m^3)
VR_{office}	ventilation rate of an office (ACH)
μ_{air}	molecular viscosity of air (kg m^{-1} s^{-1})
ρ_{air}	air density (kg m^{-3})
ρ_{bp}	density of the bioaerosol particles emitted (kg m^{-3})